Progress In Electromagnetics Research Letters, Vol. 82, 65–72, 2019

Design of an Implantable Antenna Operating at ISM Band Using Magneto-Dielectric Material

Zhihao Luan[1], Lulu Liu[2], Wei-Hua Zong[2, *], Zhejun Jin[2], and Shandong Li[1]

Abstract—A novel technique to design a wideband implantable antenna has been proposed by using magneto-dielectric material. The antenna is a half cutting of a coplanar waveguide fed antenna with symmetric geometry printed on a flexible substrate with 24 μm thickness. A piece of magneto-dielectric sheet with 0.25 mm thickness is attached on the bottom layer of the antenna to tune the antenna bandwidth. The antenna is simulated in a one-layer body phantom. Simulation shows that the antenna has a wide bandwidth covering 902–928 MHz Industrial, Scientific, and Medical (ISM) band when the body phantom is filled with muscle. There are frequency bandwidth shifts when the body phantom is filled with different tissues of skin, small intestine, and stomach, respectively. The antenna has wide bandwidth covering ISM band in these tissues. Measurement has been done in meat mince. The measured bandwidth of proposed antenna is 810–1062 MHz. The proposed antenna has a compact size of 4 mm $\times$ 12 mm $\times$ 0.274 mm suitable to be applied in capsule endoscope, wireless pacemaker, etc.

1. INTRODUCTION

Implantable biomedical devices using wireless communication have attracted much research interest in medical area due to virtues of live signal transmission and less pain to patient. These devices include wireless capsule endoscope, wireless cardiac pacemaker, glucose monitoring system, neural recording system, etc. [1–5]. Implantable antenna is an important component of an implantable wireless biomedical device to transfer data between inner body and outside body. Implantable antennas are required with miniaturized volume to reduce the physical uncomfortableness caused by the implantation inside body. The size of an ordinary antenna is inversely proportional to its working frequency.

The popularly used frequency bands of implantable devices include Industrial, Scientific, and Medical (ISM, 433.05–434.79 MHz, 902–928 MHz, and 2.4–2.4835 GHz) bands, Medical Implant Communication Services (MICS, 402–405 MHz), Ultra-Wideband (UWB, 3.1–10.6 GHz)). It is easy to design a small antenna at UWB and ISM 2.4 GHz bands. However, the human body would absorb more energy with increase of frequency when electromagnetic waves propagate inside human body. Bands of ISM 2.4 and UWB with higher frequency are difficult to transfer high quality signals. Lower bands of ISM 433 MHz and MICS with narrow frequency bands of 1.74 MHz and 3 MHz, respectively, are difficult to obtain high data rate. Therefore, ISM 902–928 MHz band is a promising band to transfer high data rate signal for implantable devises [1, 3].

Many research works have been done on compact implantable antenna design [1, 2, 4–12]. Conventional miniaturization techniques are adopted including etching slots on patch [2, 4, 5], using multiple layer stacked structure [6, 7], and meandering strip/line in folded or helical shape [1, 4, 5, 8–12]. Dielectric, magnetic, and magneto-dielectric (MD) materials with high permittivity or permeability are also used as substrates to obtain antenna size reduction [13, 14].

Received 12 November 2018, Accepted 13 January 2019, Scheduled 11 March 2019
* Corresponding author: Wei-Hua Zong (weihuazong@126.com).
[1] College of Physics, Qingdao University, Qingdao 266071, China. [2] School of Electronics and Information, Qingdao University, Qingdao 266071, China.

Since human tissues have different dielectric parameters, there are frequency shifts when an implantable antenna is embedded in different body tissues. The motive of this paper is to design a compact implantable antenna at ISM 902–928 MHz with wide bandwidth in various tissues. Two techniques are involved in this paper to design a compact and wideband implantable antenna. (1) Adopting coplanar waveguide (CPW) feeding to obtain wide bandwidth and half-cutting the CPW antenna to reduce antenna size. CPW-fed antennas are popular in UWB applications. Studies have been done on CPW-fed UWB antennas with symmetric geometry, which reveal that the half-cutting of a CPW-fed antenna with symmetric geometry results in a new antenna bandwidth [15–17]. In this paper, we use the half-cutting technique on a novel symmetric CPW (SCPW) antenna proposed by us. (2) Loading MD material to tune antenna resonant frequency and bandwidth. The adoption of MD sheet increases the antenna's effective dielectric constants and results in left-shifting of resonant frequency. MD material has been widely used in mobile antenna design to obtain size reduction and wideband width [18–23]. In this paper, the simulated first resonant frequency of an HCCPW antenna is 1048 MHz. With adding of MD at the bottom layer of the antenna, its first resonant frequency shifts to 950 MHz with -10 dB bandwidth covering 804–1500 MHz. Simulation shows that the MD loaded HCCPW antenna has a wide bandwidth in muscle, skin, stomach, and small intestine, respectively.

To validate the simulated performance of the proposed antenna, experiment measurement is required to be conducted in an environment similar to human body. In-vivo measurement in a living animal is professional and rigorous, but it involves medical surgery and costs much. In vitro measurement using meat mince or chunk is more convenient and economic than living experiment. The measured features of an antenna in meat are valuable reference for implantable applications [1, 4, 8]. In this paper, we use pork mince to measure the proposed antenna. Measurement shows that the antenna has wide bandwidth of 810–1062 MHz in pork covering ISM 902–928 MHz.

2. ANTENNA DESIGN

2.1. Antenna Configuration and Simulation Environment

Figure 1 shows antenna configuration proposed in this paper. The CPW antenna in Figure 1(a) has a geometry symmetric about XOY plane. By cutting the antenna at the symmetric plane, one half forms the HCCPW antenna as shown in Figure 1(b). The flexible Kapton polyimide with relative permittivity $\varepsilon_r = 3$, dielectric loss tangent 0.02, and thickness 24 µm is adopted as antenna substrate. A piece of flexible MD sheet with relative permittivity $\varepsilon_r = 13$, relative permeability $\mu_r = 20.7$, dielectric loss tangent $\tan\delta\varepsilon = 0.17$, magnetic loss tangent $\tan\delta\mu = 0.12$, and thickness 0.25 mm is attached at the bottom layer of the substrate as shown in Figure 1(c).

For an implantable antenna working inside human body, its resonant frequency is lower than the one working in free space. Therefore, human body is needed to be considered in antenna design. Three-dimensional Gustav voxel human body with various tissues similar to a real human being is available in some commercial softwares, such as CST Studio and FEKO. The simulation of an antenna inside the aforementioned body model can give accurate result. However, it requires large computer memory and costs much time. Simple body phantom with box shape filled with one tissue has been adopted in many articles to save computing time [5, 7, 10, 11]. Furthermore, the simulation in one-layer body phantom has a similar result to the one in a Gustav voxel human body in the frequency features characterized by scattering parameters. In this paper, we use a one-layer cubic body phantom to analyze antenna

Table 1. Body tissue dielectric parameters at 910 MHz [24].

Tissue	ε_r	σ (S/m)
Muscle	55.93	0.97
Skin (Dry)	41.35	0.87
Small Intestine	59.42	2.17
Stomach	65.03	1.19

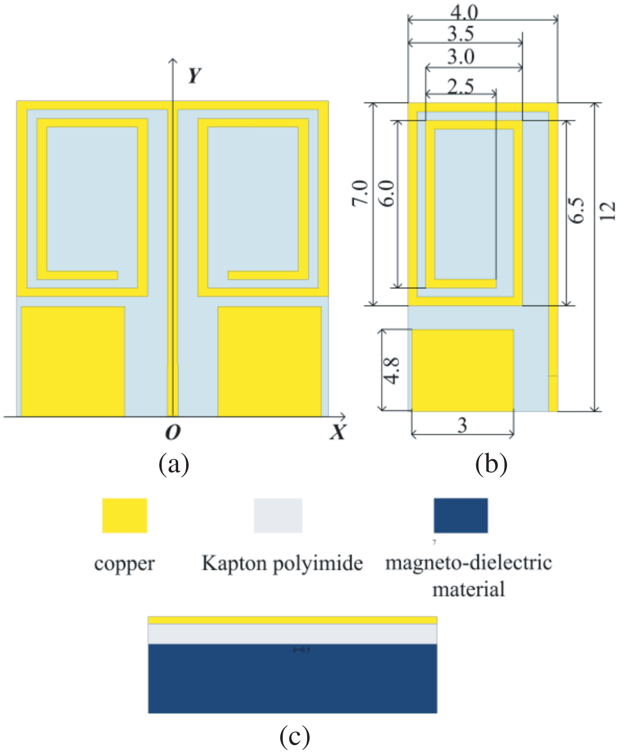

Figure 1. Antenna configuration (unit: mm). (a) Top view of SCPW antenna. (b) Top view of HCCPW antenna. (c) Side view of antenna with MD material.

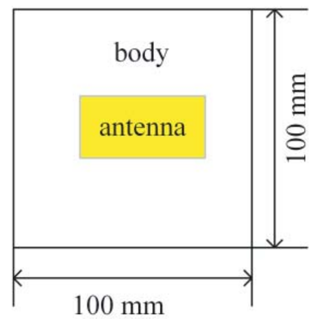

Figure 2. Simulation environment. Antenna in the center of a one-layer cubic body phantom.

frequency performance. Simulations are performed by using Ansys HFSS software. Figure 2 shows the simulation environment. The antenna is located at the center of a one-layer cubic body phantom with side length of 100 mm. The material inside the body phantom is assigned with muscle in the antenna design procedure. Other tissues of skin, small intestine, and stomach are also investigated in the following to evaluate the antenna performance. The dielectric parameters of different tissues at 910 MHz are given in Table 1 [24].

2.2. Simulation Analysis of Antenna Performance

Figure 3 shows the simulated $|S_{11}|$ of the HCCPW antenna and symmetric CPW (SCPW) antenna. As shown in the figure, the first resonant frequencies of two antennas are close to each other with 1048 MHz for the HCCPW antenna and 1023 MHz for the SCPW antenna, respectively. This means that the half cutting of the SCPW antenna has little effect on the first resonance which has been investigated in other published papers [15–17]. It is also shown in the figure that the resonant frequency of the HCCPW antenna with MD sheet is 950 MHz. The adding of MD sheet results in a frequency shift of 98 MHz to the lower band. The MD HCCPW antenna has a wide bandwidth of 804–1500 MHz with $|S_{11}| < -10$ dB.

To evaluate the antenna performance in different tissues, simulations are employed by filling the body phantom with skin, stomach, and small intestine, respectively. The dielectric parameters of these tissues are given in Table 1. Figure 4 shows simulated $|S_{11}|$ of the proposed antenna in different tissues. The resonant frequency and bandwidth are given in Table 2. The simulated $|S_{11}|$ curves vary much in different tissues. However, the antenna in each tissue has wide bandwidth covering ISM band 902–928 MHz. This means that the proposed antenna is suitable to work inside various tissues.

Radiation pattern of the proposed antenna inside body phantom filled with muscle is simulated and shown in Figure 5. As shown in the figure, the proposed antenna has an omnidirectional pattern. Table 3 gives maximum gain of the proposed antenna at frequencies of 902–928 MHz. As shown in the

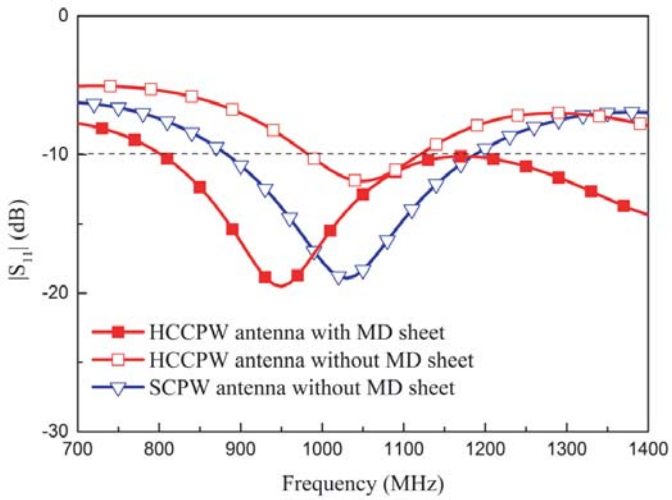

Figure 3. Simulated $|S_{11}|$ of the proposed HCCPW antenna and the SCPW antenna.

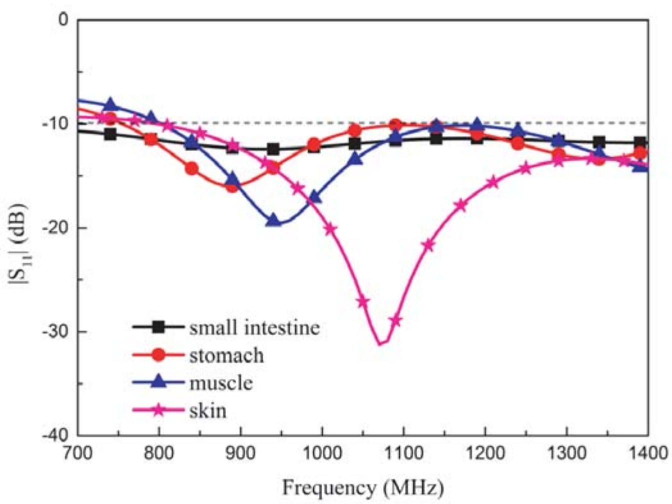

Figure 4. Simulated $|S_{11}|$ of the MD loaded HCCPW antenna in different body tissues.

Table 2. Simulated resonant frequency and bandwidth of MD loaded HCCPW antenna in different body tissues.

Tissue	Resonant Frequency (MHz)	Bandwidth (MHz)
Muscle	950	804–1500
Skin	1070	799–1500
Small Intestine	930	700–1500
Stomach	890	760–1500

figure, the proposed antenna has maximum gain higher than -30.32 dB at these frequencies, which is acceptable for an implantable antenna. SAR of the proposed antenna is also simulated and shown in Figure 6. In simulation, we compute SAR over 1 g human tissue with input power of 20 mW. As shown in Figure 6, the simulated maximum SAR is 7.1525 W/kg. To satisfy the standards IEEE C95.1-1999 of 1.6 W/kg over 1 g of tissue [25], the input power should be less than 4.4739 mW.

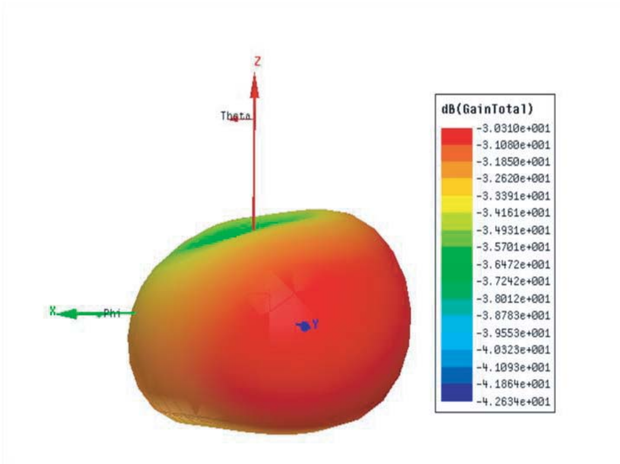

Figure 5. Simulated radiation pattern of the proposed antenna at 915 MHz.

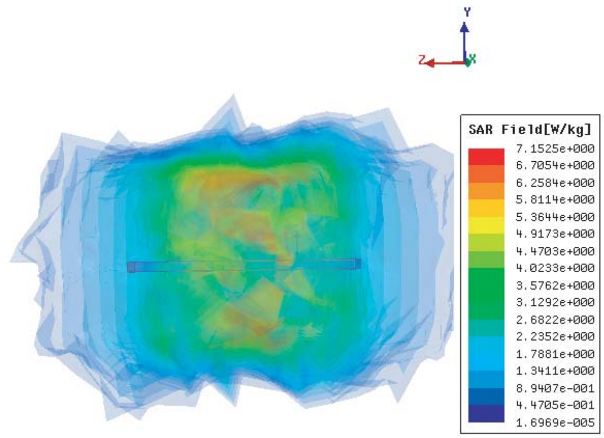

Figure 6. Simulated average SAR of the proposed antenna at 915 MHz.

Table 3. Simulated maximum gain of the proposed antenna inside body phantom filled with muscle.

Frequency (MHz)	Maximum Gain (dB)
902	−28.96
906	−29.35
910	−28.38
915	−30.32
919	−29.35
924	−29.70
928	−29.90

3. MEASUREMENT AND DISCUSSION

The proposed flexible HCCPW was fabricated and measured inside pork mince. Figure 7 shows photographs of fabricated antenna and measurement setup. The antenna under test was soldered with coaxial cable and attached with MD sheet on the bottom layer of the flexible substrates. Before arranging the antenna inside meat, it was covered with plastic film to protect the antenna and coaxial cable from corroded by the liquid inside meat. The plastic film can also avoid the short-circuit connection between

Table 4. Performance comparison of the proposed antenna with implantable antennas in published literatures.

Ref.	Antenna size (mm^3)	Bandwidth (MHz)
[1]	$13 \times 13 \times 1.27$	737–975
[26]	$11 \times 11 \times 1.27$	899–924
[27]	$25 \times 33 \times 7.6$	820–1000
[28]	$\pi(4.7)^2 \times 1.27$	900–1011
[29]	$\pi(3.5)^2 \times 15$	920–1148
[30]	$\pi(5.5)^2 \times 0.635$	800–980
This work	$4 \times 12 \times 0.274$	810–1062

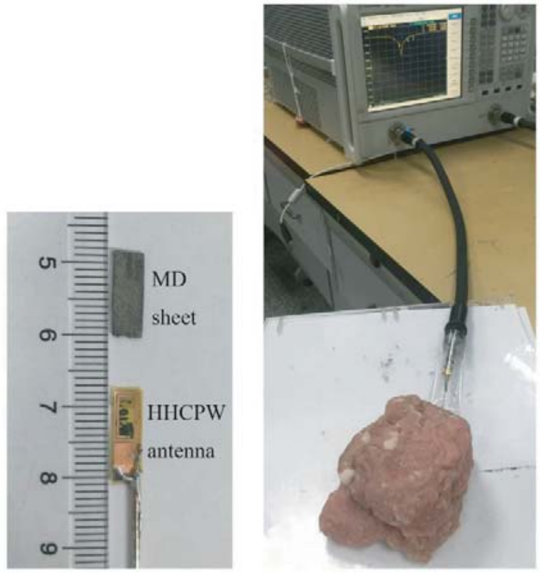

(a) (b)

Figure 7. Photograph of fabricated antenna and measurement setup. (a) Fabricated HCCPW antenna soldered with coaxial cable. (b) Measurement of antenna inside pork meat skin.

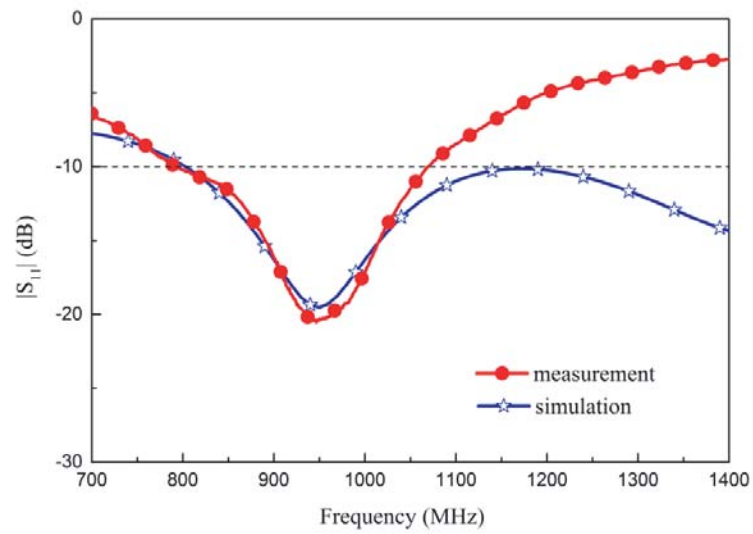

Figure 8. Measured $|S_{11}|$ of MD loaed HCCPW antenna in pork meat mince compared with simulation.

the inner and outer metals of the coaxial cable caused by liquid. The measurements were performed with an Agilent vector network analyzer N5224A.

Figure 8 shows measured $|S_{11}|$ of the proposed antenna in pork mince compared with simulation in muscle. As shown in the figure, measurement agrees well with simulation at frequencies below 1100 MHz. At frequencies above 1100 MHz, measured $|S_{11}|$ is higher than simulation. The disagreement may be caused by the air gap between the antenna and meat mince [6]. The measured bandwidth of the MD loaded HCCPW antenna is 810–1062 MHz. Table 4 gives performance comparison of the proposed antenna with implantable antennas in published literature. As shown in the table, the proposed antenna has smaller volume than those in published literature.

4. CONCLUSION

An implantable antenna has been proposed. The antenna is a half cutting of an SCPW antenna loaded with MD material. Simulation results show that the antenna has a wideband width in a one-layer body phantom filled with skin, muscle, small intestine, and stomach, respectively. Measurements have been done in meat mince. The measured bandwidth of the proposed antenna is 810–1062 MHz covering ISM band of 902–928 MHz. The proposed antenna has a small size of $4\,\mathrm{mm} \times 12\,\mathrm{mm} \times 0.274\,\mathrm{mm}$. It can be applied in implantable biomedical devices, such as capsule endoscope and wireless pacemaker.

REFERENCES

1. Xu, L. J., Y. X. Guo, and W. Wu, "Miniaturized circularly polarized loop antenna for biomedical applications," *IEEE Trans. Antennas Propag.*, Vol. 63, No. 3, 922–930, Mar. 2015.
2. Gani, I. and H. Yoo, "Multi-band antenna system for skin implant," *IEEE Microw. Wireless Comp. Lett.*, Vol. 26, No. 4, 294–296, Apr. 2014.
3. Chirwa, L. C., P. A. Hammond, S. Roy, and D. R. S. Cumming, "Electromagnetic radiation from ingested sources in the human intestine between 150 MHz and 1.2 GHz," *IEEE Trans. Biomed. Eng.*, Vol. 50, No. 4, 484–492, Apr. 2003.
4. Liu, X. Y., Z. T. Wu, Y. Fan, and E. M. Tentzeri, "A miniaturized CSRR loaded wide-beamwidth circularly polarized implantable antenna for subcutaneous real-time glucose monitoring," *IEEE Antennas Wireless Propag. Lett.*, Vol. 16, 577–580, 2017.
5. Li, H., Y. X. Guo, and S. Q. Xiao, "Broadband circularly polarised implantable antenna for biomedical applications," *Electro. Lett.*, Vol. 52, No. 7, 504–506, Jul. 2016.
6. Liu, C., Y. X. Guo, R. Jegadeesan, and S. Xiao, "In vivo testing of circularly polarized implantable antennas in rats," *IEEE Antennas Wireless Propag. Lett.*, Vol. 14, 783–786, 2015.
7. Liu, C., Y. X. Guo, and S. Qiu, "Circularly polarized helical antenna for ISM-band ingestible capsule endoscope systems," *IEEE Trans. Antennas Propag.*, Vol. 62, No. 12, 6027–6039, Dec. 2014.
8. Jung, Y. H., Y. Qiu, and S. Lee, "A compact Parylene-coated WLAN flexible antenna for implantable electronics," *IEEE Antennas Wireless Propag. Lett.*, Vol. 15, 1382–1385, 2016.
9. Li, H., Y. X. Guo, C. Liu, S. Xiao, and L. Lin, "A miniature-implantable antenna for medradio-band biomedical telemetry," *IEEE Antennas Wireless Propag. Lett.*, Vol. 14, 1176–1179, 2015.
10. Xiao, S., C. Liu, Y. Li, X. M. Yang, and X. Liu, "Small-size dual-antenna implantable system for biotelemetry devices," *IEEE Antennas Wireless Propag. Lett.*, Vol. 15, 1723–1726, 2016.
11. Xu, L. J., Y. X. Guo, and W. Wu, "Bandwidth enhancement of an implantable antenna," *IEEE Antennas Wireless Propag. Lett.*, Vol. 14, 1510–1513, 2015.
12. Alrawashdeh, R. S., Y. Huang, M. Kod, and A. A. B. Sajak, "A broadband flexible implantable loop antenna with complementary split ring resonators," *IEEE Antennas Wireless Propag. Lett.*, Vol. 14, 1506–1509, 2015.
13. Chien, T. F., C. M. Cheng, H. C. Yang, J. W. Jiang, and C. H. Luo, "Development of nonsuperstrate implantable low-profile CPW-fed ceramic antennas," *IEEE Antennas Wireless Propag. Lett.*, Vol. 9, 599–602, 2010.
14. Wang, J., J. Liu, K. Suguri, and D. Anzai, "An in-body impulse radio transceiver with implant antenna miniaturization at 30 MHz," *IEEE Microw. Wireless Comp. Lett.*, Vol. 25, No. 7, 484–486, 2015.
15. Liu, W. J. and Q. X. Chu, "Half-cut disc UWB antenna with tapered CPW structure for USB application," *Microw. Opt. Technol. Lett.*, Vol. 52, No. 6, 1380–138, Jun. 2014.
16. Sun, M. and Y. P. Zhang, "Miniaturization of planar monopole antennas for ultrawide-band applications," *Proc. Int. Workshop Antenna Technol. Small Smart Antenna Metamater. Appl.*, 197–200, Cambridge, U.K., Mar. 2007.
17. Mobashsher, A. T. and A. Abbosh, "Utilizing symmetry of planar ultra-wideband antennas for size reduction and enhanced performance," *IEEE Antennas Propag. Mag.*, Vol. 57, No. 2, 153–166, Apr. 2015.

18. Ji, J. K., W. K. Ahn, J. S. Kum, S. H. Park, G. H. Kim, and W. M. Seong, "Miniaturized T-DMB antenna with a low-loss Ni-Mn-Co ferrite for mobile handset applications," *IEEE Magnet. Lett.*, Vol. 1, 5000104–5000104, 2009.
19. Bae, S., Y. K. Hong, J. J. Lee, W. M. Seong, J. S. Kum, W. K. Ahn, and J. H. Park, "Miniaturized broadband ferrite T-DMB antenna for mobile-phone applications," *IEEE Trans. Magnetics*, Vol. 46, No. 6, 2361–2364, Jun. 2010.
20. Xia, Q., H. Su, T. Zhang, J. Li, G. Shen, H. Zhang, and X. Tang, "Miniaturized terrestrial digital media broadcasting antenna based on low loss magneto-dielectric materials for mobile handset applications," *Journal of Applied Physics*, 1–4, 2012.
21. Cheon, Y., J. Lee, and J. Lee, "Quad-band monopole antenna including LTE 700 MHz with magneto-dielectric material," *IEEE Antennas Wireless Propag. Lett.*, Vol. 11, 137–140, 2012.
22. Lee, J., Y. K. Hong, S. Bae, G. S. Abo, W. M. Seong, and G. H. Kim, "Miniature long-term evolution (LTE) MIMO ferrite antenna," *IEEE Antennas Wireless Propag. Lett.*, Vol. 10, 603–606, 2011.
23. Park, B. Y., M. H. Jeong, and S. O. Park, "A magneto-dielectric handset antenna for LTE/WWAN/GPS applications," *IEEE Antennas Wireless Propag. Lett.*, Vol. 13, 1482–1485, 2014.
24. https://www.fcc.gov/general/body-tissue-dielectric-parameters.
25. IEEE Standard for Safety Levels With Respect to Human Exposure to Radio Frequency Electromagnetic Fields, 3 kHz to 300 GHz, IEEE Standard C95.1, 1999.
26. Liu, C., Y. Zhang, and X. Liu, "Circularly polarized implantable antenna for 915 MHz ISM-band far-field wireless power transmission," *IEEE Antennas Wireless Propag. Lett.*, Vol. 17, 373–376, 2018.
27. Islam, S., K. P. Esselle, D. Bull, and P. M. Pilowsky, "Implantable compact antennas for wireless bio-telemetry: A comparative study," *The 2014 International Workshop on Antennas Technology*, 167–170, 2014.
28. Hassan, S., S. T. Waleed, K. Sana, and J. Latif, "A wideband circularly polarized implantable antenna for 915 MHz ISM-band biotelemetry devices," *IEEE Antennas Wireless Propag. Lett.*, Vol. 17, No. 8, 1473–1477, Aug. 2018.
29. Sudhakar, K., M. Nagarjuna, and R. Pandeeswari, "Design of bio implantable antenna for in body applications," *IEEE Power, Control, Communication & Computational Technologies for Sustainable Growth*, 2016.
30. Hassan, S., S. T. Waleed, K. Sana, and J. Latif, "A wideband circularly polarized implantable antenna for 915 MHz ISM-band biotelemetry devices," *IEEE Antennas Wireless Propag. Lett.*, Vol. 17, No. 8, 1473–1477, Aug. 2018.